Direct *in vivo* measurement of cochlear place coding in humans

Authors: Amit Walia, MD[1*], Amanda J. Ortmann, PhD[1], Shannon Lefler, AuD[1], Timothy A. Holden, BSE[1], Jacques A. Herzog, MD[1], Craig A. Buchman, MD[1]

[1]Department of Otolaryngology—Head and Neck Surgery, Washington University School of Medicine in St. Louis, St. Louis, Missouri, USA.

*Corresponding Author: Amit Walia, Washington University School of Medicine, Department of Otolaryngology Head & Neck Surgery, 660 S. Euclid Ave. Campus Box 8115, St. Louis, MO 63110; Phone: (314)-448-5847; Fax: (314)-453-0489; Email: amitwalia@wustl.edu

KEYWORDS: tonotopic organization, cochlea, acoustics, hearing, cochlear microphonics, intracochlear electrocochleography

ABSTRACT:

Although tonotopic place-coding in the cochlea has been extensively studied, our understanding of how the human cochlea responds *in vivo* to acoustic stimuli remains limited. We recorded acoustically-evoked intracochlear responses from 50 human subjects using a cochlear implant electrode and constructed an electrophysiology-based map using postoperative imaging to locate each electrode contact. The basal shifted frequency-place map resulting from higher stimulation more closely aligns with everyday speech levels.

The cochlea is responsible for converting sound waves into electrical impulses for hearing, by spatially separating sound waves by frequency using the basilar membrane and other soft tissues. This specificity, known as cochlear tonotopy, was first detailed by Nobel Laureate Georg von Békésy[1]. While *ex vivo* stroboscopic photography in cadavers[1, 2], *in vivo* electrophysiological and pressure recordings in animals[3, 4], and post-mortem histologically-derived retrograde tracer and imaging methods in both humans and animals[5, 6] have provided insights into the cochlear transduction process, they have limitations. These include inherent artifacts and spatial limitations resulting from surgical modifications and histologic processing[1, 7], difficulty studying cochlear amplification *ex vivo*[8], anatomical and physiological differences between animal models and humans[9], and inability to replicate dynamic biologic changes affecting passive cochlear mechanics in cadavers[10]. Therefore, little is known about how the human cochlea responds *in vivo* to various acoustic stimuli.

Existing technologies for *in vivo* electrophysiologic recordings within the human cochlea have been limited by their inability to achieve reliable and consistent intracochlear recordings and have mostly been limited to extracochlear recording sites.[11] However, intracochlear recordings could provide valuable insights into cochlear tonotopy. Cochlear implantation is an excellent model for analyzing cochlear mechanics in humans, as it involves placement of a multi-electrode array along the longitudinal axis of the cochlear lumen.

We report *in vivo*, acoustically-evoked recordings in 50 cochlear implant recipients, using the cochlear implant electrode array immediately after insertion at the round window (Fig. 1A). The array includes 22 platinum-iridium electrode contacts, spread evenly across 14.4 mm, which are individually used for recording. The implant package communicates with external recording instrumentation via a transcutaneous radiofrequency telemetry coil.

Acoustic tone-burst stimuli (250, 500, 1000, 2000, 3000, 4000 Hz) are presented and responses are recorded independently at all 22 electrodes. The electrocochleography (ECochG) responses include the cochlear microphonic (CM), auditory nerve neurophonic (ANN), transient compound action potential (CAP), and time-invariant summating potential (SP)[12]. Prior *in vivo* animal studies have shown that the CM potential reflects basilar-membrane displacement and that basilar membrane motion and auditory nerve tuning are exquisitely interrelated.[13] *In vivo* human recordings performed in this study are qualitatively similar to those recorded previously using a guinea pig model, with the unique use of multiple longitudinally inserted, intracochlear recording electrodes (Fig. 1B)[4].

To assess tonotopic frequency-position distributions, we precisely measured the location of each electrode along the array using computed tomography (CT) imaging after implantation[14]. A CT volume rendering of the electrode array within the cochlea was viewed along the mid-modiolar axis by an expert observer relative to a micro-CT atlas to measure cochlear dimensions and electrode position (Fig. 2B). The angular position (in degrees) of each electrode was measured based on the rotation about the mid-modiolar axis, with the 0° reference line starting at the round window membrane. The mean number of turns across 50 subjects was 2.6 (range, 2.2 – 2.9 turns).

Von Békésy established tonotopy and frequency-to-place mapping, with high-frequency tones peaking near the base and low-frequency tones near the apex of the basilar membrane, giving each place a distinct "best frequency" (BF). Wever and Bray II first showed electrical activity from the cochlea in response to sound in cats (i.e., Wever-Bray effect)[15]. Hallowell Davis later confirmed these responses in guinea pigs and cats, attributing them to the CM and action potential of the cochlear nerve[16]. These electrophysiological measurements combined with

von Békésy's physical and anatomical descriptions are essential for understanding human sound perception.

To determine the tonotopic distribution of BF in the human cochlea, acoustic tone-burst stimuli were presented and the fast Fourier transformation of the CM, taken as the difference between rarefaction and condensation waveforms, was evaluated at each electrode (Fig. 2A), resulting in CM tuning curves for each subject. The largest response on each curve was defined as the BF location. BF electrodes were then angle-mapped using CT reconstructions to relate the angular depth to tonotopic frequency in 50 human subjects (Fig. 2C-D).

We then compared the electrophysiologically-derived frequency-position map with organ of Corti (OC) and spiral ganglion (SG) maps by Greenwood[17] and Stakhovskaya et al[6], respectively (Fig. 2D). The modified SG and OC functions were compared using established frequency-position equations from synchrotron radiation phase-contrast imaging, providing better measurements of the helicotrema and hook region within the cochlea[18]. The electrophysiologically-derived frequency map was found to be shifted at least one octave downwards or more basal in location compared to both the OC and SG maps. Possible explanations for this shift were explored.

Can stimulus intensity explain the difference between the electrophysiologically-derived map and the SG/OC maps? Animal models have shown that higher stimulus intensities result in less sharp tuning and a shift towards lower frequencies[19, 20]. We investigated this relationship in 20 human subjects with residual hearing post-implantation, varying stimulus intensities from 36 dB HL to 91 dB HL across 250 Hz to 2000 Hz. We found that frequency tuning and BF location did not shift with decreases in stimulus intensity, although responses were limited by residual hearing (Supplementary Fig. 1-3). A patient with auditory neuropathy spectrum disorder (with present distortion product otoacoustic emissions—DPOAEs) was also tested, revealing an expected shift towards Greenwood[17] and Stakhovskaya et al.[6] with reduction in stimulus level to the limits of the equipment. Stimulation at conversational speech levels showed responses similar to high-level stimulation rather than threshold, suggesting that frequency place maps during conversation are more similar to those reported in pitch-matching experiments with cochlear implants[21] than those described by the Greenwood equation (Fig. 3).

Does the electrode array impact the frequency-position map and explain the shift seen in Fig. 2D? The impact of the electrode on the basilar membrane and the acoustic frequency-position map is poorly understood. To investigate this, we compared pitch percepts of acoustic stimuli presented to the non-implanted and implanted ear using pure tones ranging from 125 to 1250 Hz. The stimuli were balanced for loudness between both ears using a seven-point loudness scale. One ear was used as a reference with a single pure tone delivered at 250, 500, or 1000 Hz, while the other ear was presented with pure tones in random order. Subjects were asked to indicate whether the pitches presented to each ear separately sounded the same or different (Supplementary Fig. 4A). Results showed a small average difference (range, 1.30-1.65 semitones) in the acoustic perception of pure tones between both ears in two subjects (Supplementary Fig. 4B-C), suggesting that the presence of the perimodiolar electrode does not significantly explain the tonotopic basal shift observed in Fig. 2D.

Does creating an artificial cochlear 'third-window' alter the frequency-position map? Von Békésy observed the traveling wave *ex vivo* using a rubber membrane-cemented brass ring as an artificial stapes and a fenestration near the cochlear apex[1, 7, 22]. While the possibility of low-frequency stimulation artifact as a result of the fenestration has been acknowledged[1, 7, 22], the impact of the third window *in vivo* within the human cochlea is unknown. To investigate this, the

same electrode array described above was inserted into the round window of the cochlea during a translabyrinthine approach to remove a vestibular schwannoma in a human with good residual hearing. The location of the BF for frequencies between 250 Hz and 4 kHz was determined before and after the creation of the fenestration near the upper cochlear turns, and the frequency-position map did not shift with the creation of the third window, indicating that von Békésy's artificial window did not affect the estimate of the frequency-position map (Supplementary Fig. 5).

The electrophysiological findings in this study must be considered in the context of the subjects' underlying hearing loss. In mammals, outer hair cells act as cochlear amplifiers, enhancing frequency selectivity and auditory sensitivity up to 40 dB[23], while high-level stimulation causes a well-established half-octave shift of the tonotopic map toward the basal or downward frequency direction[24]. The subjects' underlying otopathology further impairs active cochlear mechanisms, resulting in a shift in the tonotopic map[25]. These factors likely account for the lack of shift in the cochlea's tonotopic place coding upon reduction in stimulus intensity in most patients. However, in the auditory neuropathy patient with preserved amplifier functions (i.e., preserved DPOAEs), the expected impact of sound intensity modulation on place coding was evident. At stimulus intensities similar to everyday listening (~70 dB HL), the frequency-position responses more closely matched the high intensity stimulus results, suggesting the electrophysiologically-derived tonotopic map may be more relevant for everyday listening and cochlear implant mapping.

Direct intracochlear electrophysiology recordings were carried out for the first time to determine the tonotopic map in humans, revealing results similar to those observed by von Békésy. Although the role of cellular motors such as the cochlear amplifier cannot be ruled out, our quantitative analysis of outer hair cell function indicates that the tonotopic place map is basally or downward shifted at suprathreshold stimulus levels, more closely resembling typical hearing conditions than the Greenwood 1990 model[17]. Clinical studies that utilize electrophysiological recordings to evaluate patient-specific frequency mapping in cochlear implant recipients could help improve frequency representation and potentially enhance their hearing outcomes.

REFERENCES:

1. Von Békésy, G. & Peake, W.T. Experiments in Hearing. *The Journal of the Acoustical Society of America* 88, **2905** (1990).

2. Von Békésy, G. Travelling Waves as Frequency Analysers in the Cochlea. *Nature* **225**, 1207-1209 (1970).

3. Müller, M. The cochlear place-frequency map of the adult and developing Mongolian gerbil. *Hearing research* **94**, 148-156 (1996).

4. Tasaki, I., Davis, H. & Legouix, J.P. The Space□Time Pattern of the Cochlear Microphonics (Guinea Pig), as Recorded by Differential Electrodes. *The Journal of the Acoustical Society of America* **24**, 502-519 (1952).

5. Liberman, M.C. Single-neuron labeling in the cat auditory nerve. *Science* **216**, 1239-1241 (1982).

6. Stakhovskaya, O., Sridhar, D., Bonham, B.H. & Leake, P.A. Frequency map for the human cochlear spiral ganglion: implications for cochlear implants. *Journal of the Association for Research in Otolaryngology* **8**, 220-233 (2007).

7. Von Békésy, G. *Zur Theorie des Hörens: Die Schwingungsform der Basilarmembran* (Éditeur inconnu, 1928).

8. Brownell, W.E., Bader, C.R., Bertrand, D. & de Ribaupierre, Y. Evoked mechanical responses of isolated cochlear outer hair cells. *Science* **227**, 194-196 (1985).

9. Nadol, J.B., Jr. Comparative anatomy of the cochlea and auditory nerve in mammals. *Hear Res* **34**, 253-266 (1988).

10. Zhang, Y., *et al.* Prestin derived OHC surface area reduction underlies age-related rescaling of frequency place coding. *Hear Res* **423**, 108406 (2022).

11. Fitzpatrick, D.C., *et al.* Round window electrocochleography just before cochlear implantation: relationship to word recognition outcomes in adults. *Otology & neurotology* **35**, 64-71 (2014).

12. Eggermont, J.J. Cochlea and auditory nerve. *Handbook of clinical neurology* **160**, 437-449 (2019).

13. Ruggero, M.A., Narayan, S.S., Temchin, A.N. & Recio, A. Mechanical bases of frequency tuning and neural excitation at the base of the cochlea: comparison of basilar-membrane vibrations and auditory-nerve-fiber responses in chinchilla. *Proc Natl Acad Sci U S A* **97**, 11744-11750 (2000).

14. Teymouri, J., Hullar, T.E., Holden, T.A. & Chole, R.A. Verification of Computed Tomographic Estimates of Cochlear Implant Array Position: A Micro-CT and Histologic Analysis. *Otology & Neurotology* **32** (2011).

15. Wever, E.G. & Bray, C.W. Action Currents in the Auditory Nerve in Response to Acoustical Stimulation. *Proceedings of the National Academy of Sciences* **16**, 344-350 (1930).

16. Davis, H. The Electrical Phenomena of the Cochlea and the Auditory Nerve. *The Journal of the Acoustical Society of America* **6**, 196-197 (1935).

17. Greenwood, D.D. A cochlear frequency-position function for several species--29 years later. *The Journal of the Acoustical Society of America* **87**, 2592-2605 (1990).

18. Helpard, L., *et al.* An Approach for Individualized Cochlear Frequency Mapping Determined From 3D Synchrotron Radiation Phase-Contrast Imaging. *IEEE transactions on bio-medical engineering* **68**, 3602-3611 (2021).

19. Versteegh, C.P.C. & van der Heijden, M. Basilar membrane responses to tones and tone complexes: nonlinear effects of stimulus intensity. *Journal of the Association for Research in Otolaryngology* **13**, 785-798 (2012).

20. de Boer, E. & Nuttall, A.L. The mechanical waveform of the basilar membrane. III. Intensity effects. *The Journal of the Acoustical Society of America* **107**, 1497-1507 (2000).

21. Peters, J.P.M., Bennink, E. & van Zanten, G.A. Comparison of Place-versus-Pitch Mismatch between a Perimodiolar and Lateral Wall Cochlear Implant Electrode Array in Patients with Single-Sided Deafness and a Cochlear Implant. *Audiology and Neurotology* **24**, 38-48 (2019).

22. Von Békésy, G. Concerning the pleasures of observing, and the mechanics of the inner ear." Nobel Lecture, December 11 (1961).

23. Liberman, M.C., *et al.* Prestin is required for electromotility of the outer hair cell and for the cochlear amplifier. *Nature* **419**, 300-304 (2002).

24. Ruggero, M.A., Rich, N.C. & Recio, A. The effect of intense acoustic stimulation on basilar-membrane vibrations. *Auditory Neuroscience* **2**, 329-345 (1996).

25. Robles, L. & Ruggero, M.A. Mechanics of the mammalian cochlea. *Physiological reviews* **81**, 1305-1352 (2001).

AUTHOR CONTRIBUTIONS:
A.W. designed the study, participated in data collection and analyses, drafted and approved the final version of this paper. C.A.B. designed the study, participated in data collection, drafted and approved the final version of this paper. T.A.H., S.M.L., J.A.H., and A.J.O. participated in data collection, manuscript preparation, and approved the final version of this manuscript.

COMPETING INTERESTS:
C.A.B. serves as a consultant for Advanced Bionics, Cochlear Ltd., Envoy, and IotaMotion and has equity interest in Advanced Cochlear Diagnostics. J.A.H. serves as a consultant for Cochlear Ltd. For the remaining authors, none were declared.

ADDITIONAL INFORMATION:
AW was supported by NIH/NIDCD institutional training grant T32DC000022. CAB is supported by Department of Defense grant W81XWH19C0054 and NIH/NIDCD grant DC020936-01.

DATA AVAILABILITY:
The data that support the findings of this study are being made available on Zenodo.

CODE AVAILABILITY:
The code to analyze the data and generate the figures of this manuscript are being made available on GitHub.

FIGURES:

Fig. 1. Measurement of live cochlear place coding in humans. (A) An insert earphone was placed into the external auditory canal which was then connected to a sound processor to generate the acoustic stimulus. The surgical site for placement of the recording electrode was then prepared in a sterile-fashion and the round window of the cochlea was exposed using a post-auricular incision and mastoidectomy. The receiver-stimulator for the implant electrode was placed in a subperiosteal pocket and the perimodiolar electrode array was inserted into the round window, within scala tympani according to the manufacturer specification. Following insertion of the electrode, a telemetry coil was placed over the skin in alignment with the cochlear implant antenna which allowed for direct measurement from each of the 22 electrodes on the array in response to acoustically-generated stimulus. The complex signal response measured from each electrode consisted of the electrical activity from outer and inner hair cells and the spiral ganglion (inset). Post-hoc analysis of the ongoing response was performed off-line to separate the hair cell and neural components of the response. A significant response was defined as one whose magnitude exceeded the noise floor by 3 standard deviations. (B) Acoustic stimuli were presented at 250, 500, 1000, 2000, 3000, and 4000 Hz and *in vivo* recordings were made at all 22 electrode contacts. The responses at all even electrodes are shown in the color-matched figure on the right panel where the most-apical electrode (electrode **a**) shows a large response for the 250 Hz stimulus and the responses along more basal electrodes show larger responses for higher frequencies. The electrophysiological properties of the human cochlea are demonstrated with greater electrical responses to higher frequencies at the basal end and larger responses to lower frequencies at the apex. These recordings were performed in 50 subjects, showing similar findings.

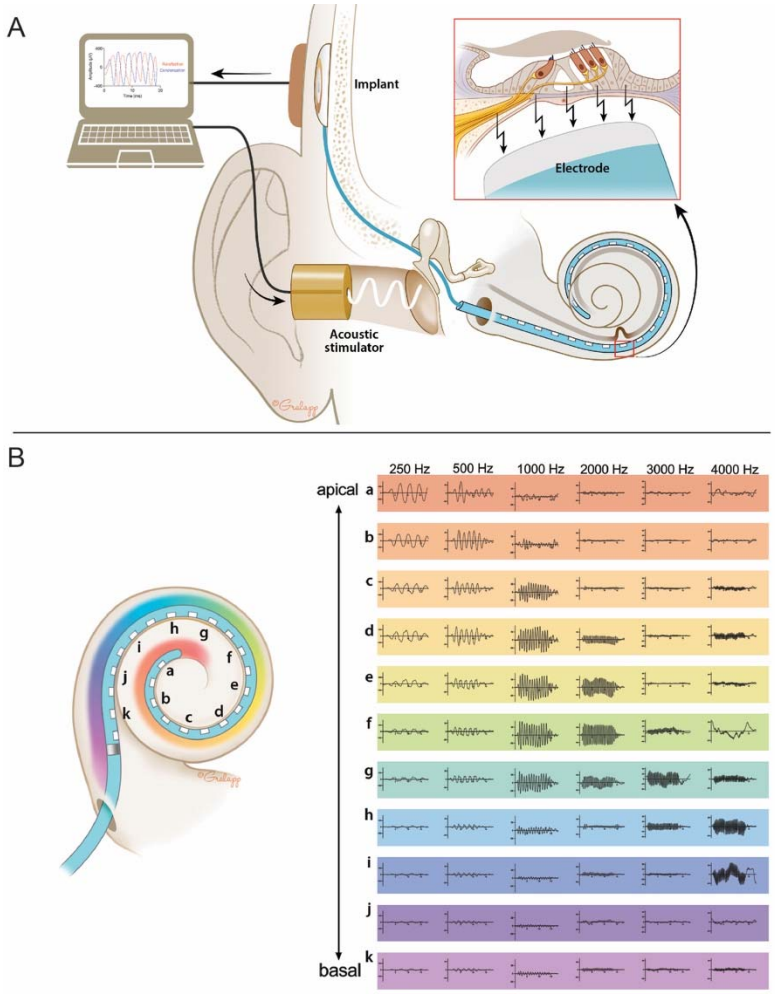

Fig. 2. Electrophysiologically-derived frequency-position map. (A) The difference curve was calculated by subtracting rarefaction from condensation phase stimuli. The difference consists primarily of the cochlear microphonic or the ongoing cyclical signal due primarily to the receptor current of outer hair cells. The ongoing portion of the response was selected for fast Fourier transformation and the amplitude of the response to the particular stimulus frequency was determined. Here, 500 Hz is shown for one subject. This was performed across all 22 electrodes in response to 500 Hz and the largest amplitude response was defined as the best frequency (BF) location for that particular frequency (e.g., $BF_{500\ Hz}$). In this subject, the BF was at electrode-18 for 500 Hz. (B) Computed tomography (CT) imaging and 3D reconstructions were performed postoperatively to identify the individual electrodes and visualize the adjacent soft tissue anatomy. To determine the position of each electrode, the CT image of each subject's cochlea was viewed along the mid-modiolar axis and the round window was marked at the 0° at the start of the cochlear canal since all insertions were performed at the round window. The angular position was then measured based on the rotation at the mid-modiolar axis. For this subject, the BF was at electrode-18 which was measured at 364° within the subject's cochlea. Here, the frequency-position relationship using electrophysiologic responses was determined for 500 Hz. (C) The same methodology described above was performed for 1000, 2000, 3000 and 4000 Hz to develop a frequency-position function for the individual subject's cochlea using the electrophysiologic responses and CT imaging for the location of each electrode. (D) These electrophysiologic measurements were repeated in 49 additional subjects and CT imaging was performed to identify the precise location of each BF to generate a cumulative frequency-position function for the electrophysiologically-derived map (ECochG map). Error bars are +/- 2 standard deviations (SD). This was compared to organ of Corti (OC) and spiral ganglion (SG) maps as established by Greenwood and Stakhovskaya et al., respectively. The ECochG map in this study is at least one octave shifted downward in frequency or more basal in location compared to both the SG and OC maps. The OC map is also shown across various size cochleae (i.e., 2.1 and 2.9 turns), illustrating that the size variability cannot account for the difference between the ECochG map and the OC map.

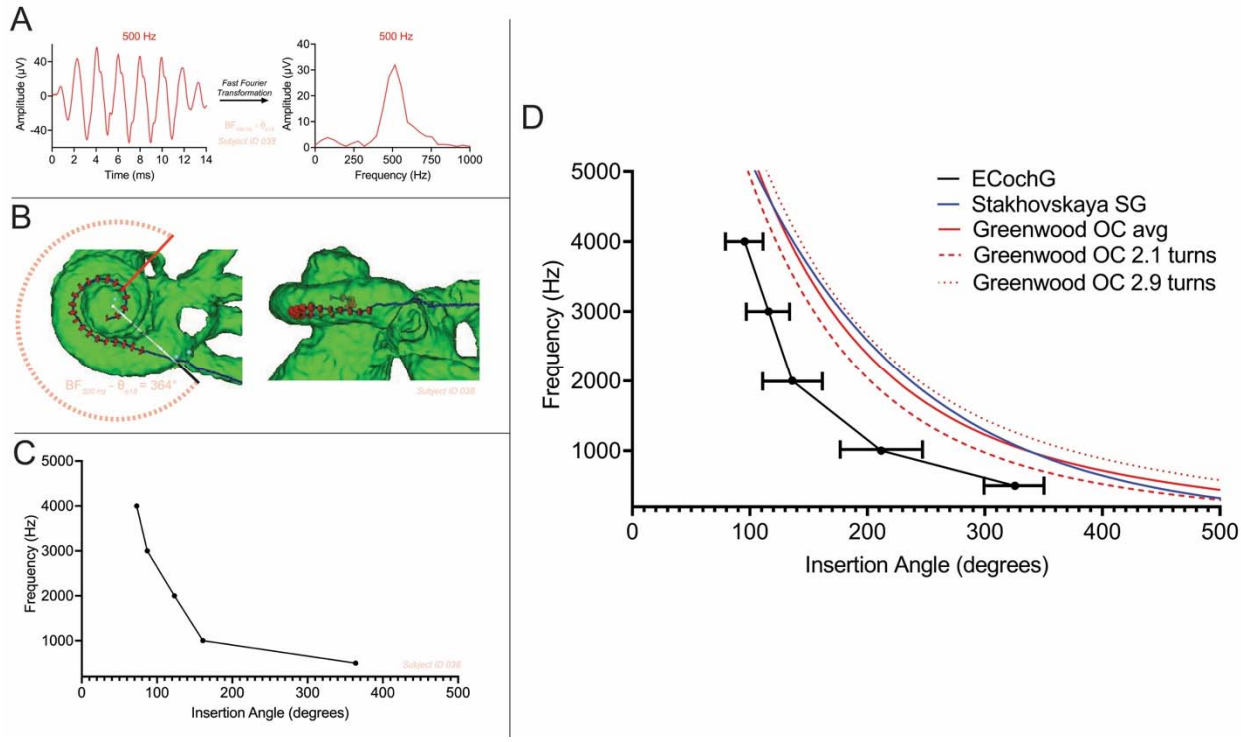

Fig. 3. Impact of intensity stimulus on frequency-position map. A subject with auditory neuropathy spectrum disorder was tested, a condition known to have substantial preservation of cochlear hair cell function as evidenced by present distortion-product otoacoustic emissions (2-8 kHz) and cochlear microphonics on auditory brainstem response testing. This was carried out to determine whether stimulus intensity modulation could account for the basal shifted tonotopic tuning derived from the intracochlear electrocochleography (Fig. 2D). Reduction in stimulus level to the limits of the equipment revealed the expected shift in an apical direction for all four frequencies tested: (A) 1000 Hz, (B) 2000 Hz, (C) 3000 Hz, and (D) 4000 Hz. The amplitude shown here are the fast Fourier transformation amplitudes of the difference response, which is primarily representative of the cochlear microphonic tuning curve (i.e., outer hair cell tuning curve). The asterisk (*) represents the best frequency (BF) electrode for each frequency and particular stimulus intensity. The stimulus levels more similar to conversational speech showed responses similar to those seen at highest stimulation level rather than those at threshold, which emphasizes that the frequency-position maps during conversation are more similar to the high-intensity electrophysiologically-derived map rather than that described by the Greenwood equation.

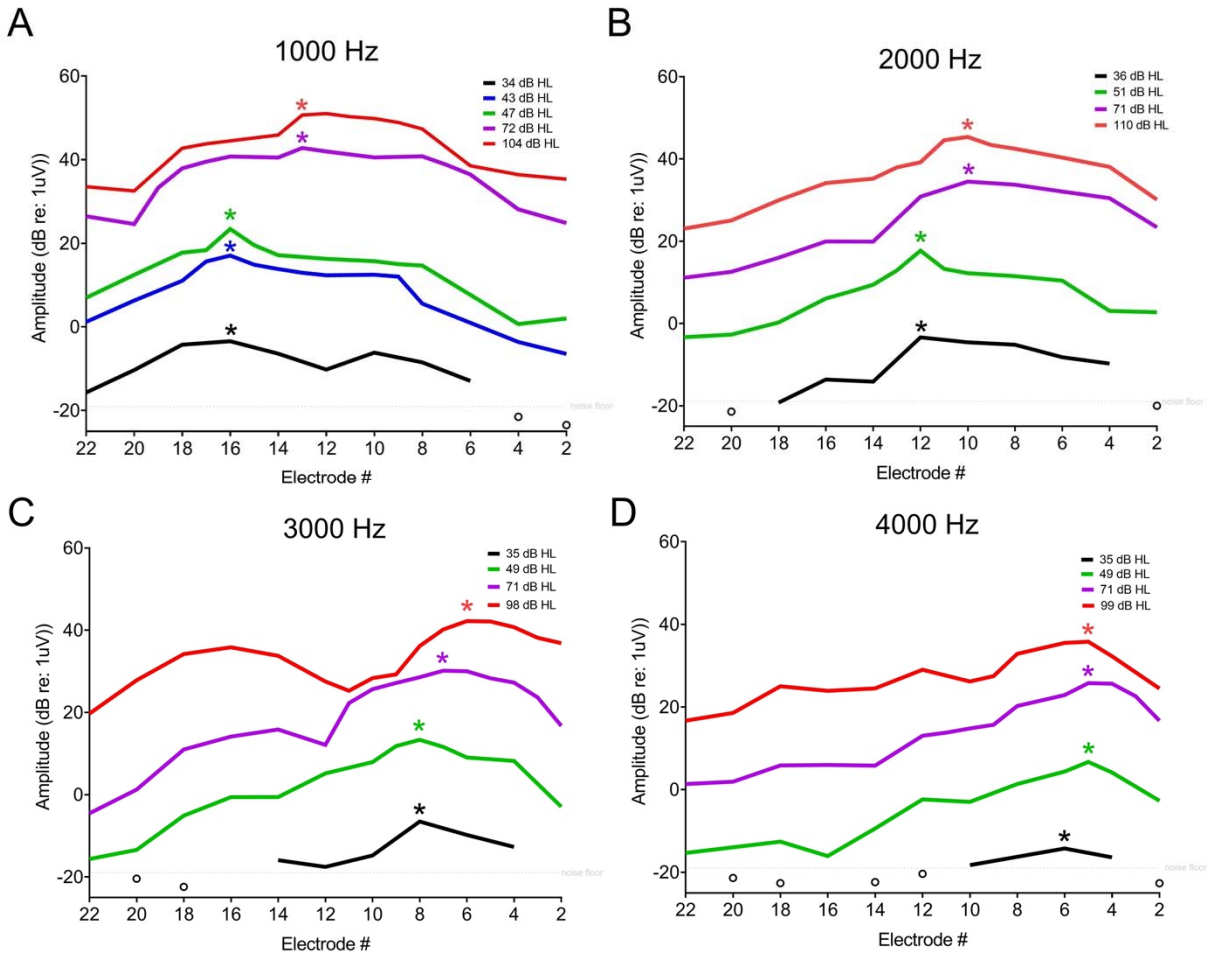

Methods

Study Design

Objectives of the study were to (i) describe the frequency-position function using the electrophysiologic recordings and compare with previously derived organ of Corti and spiral ganglion tonotopic maps of the human cochlea and (ii) investigate whether stimulus intensity, presence of the recording electrode, and creation of a third window could impact the frequency-position map.

Fifty human subjects were recruited to participate in this study under Institutional Review Board (IRB) approval (Washington University in St. Louis IRB #202007087). Subjects were considered for recruitment if they were undergoing cochlear implantation. Eligible subjects were adults with residual low-frequency hearing prior to surgery, defined as low-frequency pure tone average of 125, 250 and 500 Hz ≤ 60 dB HL. Subjects who had middle ear pathology or those undergoing revision surgery were excluded. Additionally, subjects who did not have a patent external auditory canal were excluded as the acoustic stimulus was delivered via air conduction. A demographic summary of all subjects is presented in table S1.

Surgical Technique for Electrode Placement

Five surgeons performed the operations and recordings with assistance of an audiologist. Surgery included a standard post-auricular incision and mastoidectomy to access the temporal bone. A posterior tympanotomy is used to access the cochlea and a round window related approach to scala tympani is used for the electrode array insertion. The receiver-stimulator is placed in a subperiosteal pocket. A perimodiolar electrode array was used for all insertions (CI632; Cochlear Corp., Sydney, NSW, Australia).

Intracochlear Electrophysiologic Measurements

Prior to sterile preparation of the surgical site, an ER3-14A insert earphone (Etymotic, Elk Grove Village, IL, United States) is placed into the external auditory canal. After the electrode has been inserted into the cochlea, a telemetry coil is placed over the skin in alignment with the cochlear implant antennae via a sterile ultrasound drape. All 22 electrodes along the electrode array are conditioned with reference to the case ground. Tone burst stimuli of 250-, 500-, 1000-, 2000-, 3000-, and 4000-Hz were independently delivered in condensation and rarefaction starting phases, with at least 30 repetitions per phase. The 250-, 500-, 1000-, 2000-, 3000-, and 4000-Hz stimuli were delivered at 108-, 99.5-, 98-, 104-, 102-, and 101-dB HL, respectively, which was based on the maximal output of the speaker. The stimulus duration was 14 ms with rise and fall time of 1 ms, shaped by a Blackman window. The recording epoch was 18 ms, starting 1 ms before the stimulus onset, with a sampling rate of 20 kHz. Responses were recorded across all 22 electrodes along the array.

Electrophysiology Signal Analysis

The electrophysiologic responses were processed offline and stored as condensation and rarefaction phases. Using MATLAB R2020a (MathWorks Corp., Natick, MA, United States) with custom software procedures, the difference curve was calculated by subtracting rarefaction form condensation phase stimuli. From the difference curve, the ongoing portion of the response was selected for fast Fourier transformation (FFT) and the amplitude of the response to the

various stimulus frequencies was determined. These amplitudes were used to generate cochlear microphonic (CM) tuning curves for each individual frequency across the entire electrode array. As described in previous studies, a significant response was defined as one whose magnitude exceeded the noise floor by 3 standard deviations [1-3]. The noise floor was ~0.3 μV for this series of recordings.

Computed Tomography Imaging of Electrode Position

The position of all 22 electrodes along the electrode array were determined in all patients using computed tomography (CT) scans and 3D reconstructions. The platinum iridium contacts affect the CT image by creating a bloom effect which makes it difficult to identify the individual electrodes and adjacent soft tissue anatomy. A validated technique to overcome this artifact was used to precisely identify the position of the implanted electrodes within the cochlea [4-6]. Each subject's pre-implant CT image voxel space which is optimized for anatomical detail is co-registered with their post-implant CT image space which is optimized for resolution of the electrode. The electrode contacts are identified and then segmented from the post-implant image data and copied onto the pre-implant image space to generate a composite image of the electrode within an individual subject's cochlea. The scalar position of the electrode array and the individual electrode contacts is visualized by aligning the composite CT volume to that of a high-resolution micro-CT cochlear atlas derived from cadaveric temporal bones; this is used to infer the location of the soft tissue structures within the cochlea not resolved by CT (e.g., basilar membrane). To determine the position of each electrode, the composite CT volume of each subject's cochlea is viewed along the mid-modiolar axis. The round window is marked as the 0° starting point of the cochlear canal as all electrode insertions were performed using a round window-related approach. The angular position of each electrode is then measured based on rotation about the mid-modiolar axis from the 0° start point.

Electrophysiologically-Derived Frequency-Position Map

The best frequency (BF) is defined as that electrode along the array (i.e., cochlear place on the basilar membrane) that responds maximally to a particular frequency stimulus. The CT-derived angle-based mapping of the BF electrode for each stimulus was used to create a tonotopic map in all 50 subjects. This electrophysiologically-derived map was then compared to derived organ of Corti and spiral ganglion frequency-position map functions [7-9].

Stimulus Intensity and the Frequency-Position Map

The impact of stimulus intensity on the frequency tuning of the cochlea was evaluated using electrophysiologic recordings in eleven subjects (20 of the 50 patients above and 1 with auditory neuropathy spectrum disorder). Once the BF electrode was identified at the highest intensity stimulus (as defined by the limit of the speaker) for a particular frequency, the stimulus intensity was decreased in 5-dB increments. These measurements were performed at the BF electrode and immediately adjacent electrodes to determine whether there would be an apical or basal shift of the BF with decreasing stimulus intensity. A single sweep was performed for these measurements and the noise floor for these measurements was ~1.0 μV. The rest of the stimulus and recording parameters including the signal processing was identical to that described above.

To model the impact of stimulus intensity modulation on BF place in a cochlea with substantially preserved hair cell function, a patient with auditory neuropathy spectrum disorder was identified.

This patient had both present distortion-product otoacoustic emissions (DPOAEs) between 2 and 8 kHz and auditory brainstem response waveforms consistent with a CM and absent neural waveforms. After electrode array placement, measurements were made across every electrode along the array at high-intensity, conversation-level intensity (~70 dB HL) and near threshold (~20-30 dB HL) for 4 stimulus frequencies (1000-, 2000-, 3000, and 4000-Hz). Thirty sweeps were performed for this subject. The CM tuning curves were generated for varying intensities and frequencies.

Pitch Discrimination Testing with Electrode Array

To study the impact of the electrode on the frequency-position map, acoustic pitch-discrimination was compared between ears in two unilateral cochlear implant subjects. The cochlear implant processor was not used for this portion of the testing. Both subjects had their implant for less than 6 months and had residual hearing preserved in the implant ear after implantation (postoperative low-frequency pure tone average of 125-, 250-, and 500-Hz <60 dB HL). Additionally, both subjects had similar residual hearing in the non-implanted ear. Each participant attended two sessions, with at least two weeks between sessions. Both sessions were approximately 2 hours in length and were conducted in a double-walled sound booth. Audiometric air conduction thresholds from 250 Hz to 8 kHz were obtained using insert earphones for each ear. The acoustic stimuli were first balanced for loudness at the tested frequency between ears using a seven-point loudness scale from inaudible to uncomfortably loud in order to identify that the stimulus intensity was comfortable in both ears [10]. Next, the non-implanted ear was kept at a stimulus intensity that was determined as comfortable and the acoustic stimulus intensity of the implanted ear was adjusted at 5-dB increments and then 1-dB increments to identify the precise stimulus level where the tone sounded similar in both ears. This process was repeated three times for each individual frequency tested (i.e., 250-, 500-, 1000-Hz) and the median value was used for the pitch-discrimination portion of the testing. After loudness balancing at a comfortable level, the non-implant ear was then held constant at the tested frequency (i.e., 250-, 500-, 1000-Hz) and the implant ear was presented with acoustic pure tones ranging 2 octaves from the non-implant ear's constant frequency in a random order. There was a total of 80 individual presentations of the various pure tones. The subject was then asked to indicate whether both pitches presented to each ear separately sounded the 'same' or 'different'. The outliers were defined where the subject had one response that was different from the other 4 responses, which is commonly noted as a component of fatigue in pitch-discrimination testing [11]. This testing was then repeated at a separate session, where the implant ear frequency was held constant and the non-implant ear frequency was varied.

Third Window and the Frequency-Position Map

Previous *ex vivo* experiments on tonotopy, including von Békésy's experiments, have used a fenestration of the cochlear lumen to directly observe or record the traveling wave. The potential impact of this artifact on the frequency-position map has not been previously studied. The impact of the third window on electrophysiologic recordings was assessed in a human subject with excellent residual hearing who was undergoing a translabyrinthine craniotomy (which intentionally destroys the residual hearing) for resection of a vestibular schwannoma. Prior to labyrinthine resection, the cochlea was approached and the same type of device was inserted in a manner, identical to that described above. BF was identified along the array for 250-, 500-, 1000-, 2000-, 3000-, and 4000-Hz at the maximum intensity output of the speaker and the signals were

processed as discussed above. After generating the CM tuning curves, a 1-mm diamond burr was used to create a fenestration near the upper cochlear turns and the CM tuning curves were generated again to determine whether the third window had an impact on the location of the BF. The implant was removed and surgery proceeded without inciedent. The CM tuning curves were generated for the individual frequencies, comparing pre- and post-fenestration of a third window.

1. Walia, A., *et al.* Promontory Electrocochleography Recordings to Predict Speech-Perception Performance in Cochlear Implant Recipients. *Otology & neurotology : official publication of the American Otological Society, American Neurotology Society [and] European Academy of Otology and Neurotology* **43**, 915-923 (2022).

2. Fitzpatrick, D.C., *et al.* Round window electrocochleography just before cochlear implantation: relationship to word recognition outcomes in adults. *Otology & neurotology : official publication of the American Otological Society, American Neurotology Society [and] European Academy of Otology and Neurotology* **35**, 64-71 (2014).

3. Calloway, N.H., *et al.* Intracochlear electrocochleography during cochlear implantation. *Otology & neurotology : official publication of the American Otological Society, American Neurotology Society [and] European Academy of Otology and Neurotology* **35**, 1451-1457 (2014).

4. Holden, L.K., *et al.* Factors affecting open-set word recognition in adults with cochlear implants. *Ear and hearing* **34**, 342-360 (2013).

5. Teymouri, J., Hullar, T.E., Holden, T.A. & Chole, R.A. Verification of computed tomographic estimates of cochlear implant array position: a micro-CT and histologic analysis. *Otology & neurotology : official publication of the American Otological Society, American Neurotology Society [and] European Academy of Otology and Neurotology* **32**, 980-986 (2011).

6. Skinner, M.W., *et al.* In vivo estimates of the position of advanced bionics electrode arrays in the human cochlea. *The Annals of otology, rhinology & laryngology. Supplement* **197**, 2-24 (2007).

7. Greenwood, D.D. A cochlear frequency-position function for several species--29 years later. *The Journal of the Acoustical Society of America* **87**, 2592-2605 (1990).

8. Stakhovskaya, O., Sridhar, D., Bonham, B.H. & Leake, P.A. Frequency map for the human cochlear spiral ganglion: implications for cochlear implants. *Journal of the Association for Research in Otolaryngology : JARO* **8**, 220-233 (2007).

9. Helpard, L., *et al.* An Approach for Individualized Cochlear Frequency Mapping Determined From 3D Synchrotron Radiation Phase-Contrast Imaging. *IEEE transactions on bio-medical engineering* **68**, 3602-3611 (2021).

10. Blamey, P.J. & Martin, L.F. Loudness and satisfaction ratings for hearing aid users. *J Am Acad Audiol* **20**, 272-282 (2009).

11. Elliott, D.N., Sheposh, J. & Frazier, L. Effect of Monaural Fatigue upon Pitch Matching and Discrimination. *The Journal of the Acoustical Society of America* **36**, 752-756 (1964).